Adaptively Directional Wireless Power Transfer for Large Sensor Networks

Zhe Wang, Lingjie Duan
Pillar of Engineering Systems and Design
Singapore University of Technology and Design, Singapore
Email: zhe_wang@sutd.edu.sg; lingjie_duan@sutd.edu.sg

Rui Zhang
Department of Electrical & Computer Engineering
National University of Singapore
Email: elezhang@nus.edu.sg

***Abstract*—Wireless power transfer (WPT) prolongs the lifetime of wireless sensor network by providing sustainable power supply to the distributed sensor nodes (SNs) via electromagnetic waves. To improve the energy transfer efficiency in a large WPT system, this paper proposes an adaptively directional WPT (AD-WPT) scheme, where the power beacons (PBs) adapt the energy beamforming strategy to SNs' locations by concentrating the transmit power on the nearby SNs within the efficient charging radius. With the aid of stochastic geometry, we derive the closed-form expressions of the distribution metrics of the aggregate received power at a typical SN. We analyze the optimal charging radius that maximizes the average received power. It is shown that both the optimal charging radius and maximized average received power decrease with the increased density of the SNs and the energy beamwidth. Finally, we show that the optimal AD-WPT can significantly improve the energy transfer efficiency compared to the traditional omnidirectional WPT.**

I. Introduction

Wireless sensor networks (WSNs) consist of small-size, low-power and distributed sensor nodes (SNs) to monitor physical or environmental conditions [1]. WSNs are often required to operate for long periods of time, but the network lifetime is constrained by the limited battery capacity and costly battery replacement at SNs. To extend the network lifetime, it is desirable to recharge the SNs in an undisruptive and energy efficient way.

RF-enabled wireless power transfer (WPT) [2] provides a controllable and sustainable power supply to sensor network by charging SNs via electromagnetic (EM) waves [3]. There are mainly two types of WPT: omnidirectional WPT [6]–[9] and directional WPT [10]–[12]. For omnidirectional WPT, the energy transmitter or so-called power beacon (PB) broadcasts the EM waves equally in all directions regardless of the locations of the energy receivers. According to the law of conservation of energy, the energy radiated in the direction of energy receivers accounts for only a small fraction of the total radiated power. Since the EM waves fade rapidly over distance, it may require excessively high transmit power to charge an energy receiver via omnidirectional WPT, which may not be energy efficient. In contrast, for directional WPT with antenna arrays, the PB concentrates the radiated energy in the directions of the energy receivers, i.e., via energy beamforming, which enhances the power intensity in the intended directions and thus improves the energy transfer efficiency.

Directional WPT has been addressed in [10]–[12]. In [10], energy beamforming is studied in a broadcast network where the transmitter steers the energy beams towards the receivers to maximize their received power. In [11], energy beamforming is designed in a MIMO broadcast network jointly with information beamforming, where the transmitter adjusts the beam weights to maximize the received power and information rate at different receivers. In [12], each mobile node in a cellular network is charged by its nearest PB via energy beamforming. For the simplicity of analysis, only the received power from the nearest PB is considered and the received energy from all other PBs is omitted in [12].

For a large-scale WSN, there are mainly two challenges in designing the directional WPT. On the *PB-side*, it is challenging to adapt the energy beamforming strategy to the random locations of the SNs, e.g., to decide which SNs to serve, how many beams to generate and the beamwidth of each beam, etc. On the *SN-side*, it is difficult to analyze the aggregate received power from a large number of PBs in the network, where the radiation directions and energy intensity may vary for each PB.

In this paper, we aim at tackling the above two challenges. The paper structure and contributions are given as follows.

- *Energy-efficient AD-WPT scheme to power a large-scale sensor network*: To address the PB-side challenge, we propose an adaptively directional WPT (AD-WPT) scheme in a large-scale sensor network in Section II, where the energy beamforming of the PBs is adaptive to the nearby SN locations within the energy-efficient charging radius.
- *Analysis of harvested power using stochastic geometry*: To address the SN-side challenge, in Section III, we successfully derive the closed-form expressions of distribution metrics of the aggregate received power at a typical SN from the large-scale PB network using stochastic geometry [4], [5].
- *Optimal AD-WPT for average power maximization*: To achieve the optimal AD-WPT, we design the optimal charging radius to maximize the average received power of the SNs in Section IV. We show that both the optimal charging radius and maximized average received power decrease with the increased beamwidth and SN density.

In Section V, the numerical results are shown and discussed.

This work is supported by the SUTD-MIT International Design Centre (IDC) Grant (Project Number: IDSF1200106OH), the SUTD-ZJU Joint Collaboration Grant (Project Number: SUTDZJU/ RES/03/2014) and SUTD Start-Up Research Grant (Project Number: SRG ESD 2012 042).

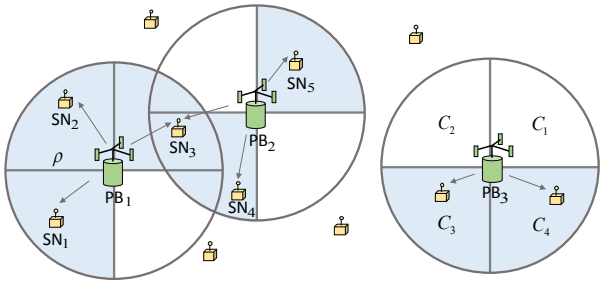

Fig. 1. System model of AD-WPT (illustrative example of $N = 4$). The circular areas with radius ρ are the charging regions of the PBs. The shaded sectors in the charging regions are the active sectors of the PBs.

Finally, conclusions are drawn in Section VI.

II. System Model

We consider a wireless charging network in Fig. 1, where a PB network wirelessly charges an SN network via energy beamforming. Each PB radiates EM waves with wavelength ν using transmit power P_p. The PBs and SNs follow two independent homogeneous Poisson Point Processes (PPPs) $\Phi_p = \{X_i\}$ and $\Phi_s = \{Y_j\}$ with density λ_p and λ_s, respectively, where X_i and Y_j represent the coordinates of the PBs and SNs in $\mathbb{R}^2$ plane.

A. AD-WPT Scheme

Due to the fast attenuation of the radio power over the distance, it is more energy efficient for the PBs to focus the energy to charge the nearby SNs. With antenna arrays, a PB is able to form an energy beam in a certain direction or generate multiple beams simultaneously towards different directions [13]. In this subsection, we propose an AD-WPT scheme where the PBs adapt the beamforming strategy to the random locations of the SNs.

To decide which SNs to charge, we define *charging region* as a circular region centered at each PB with *charging radius* ρ, as shown in Fig. 1. Each charging region is divided into N equal sectors $C_1, \cdots, C_N$, where N is usually a small positive integer due to physical constraint of antenna design. We consider that a PB is aware of the existence of the SNs inside each of its sectors, e.g., via the SN feedback over control channels. A sector is considered to be active if at least one SN falls into this sector. Denote M as the random number of active sectors of a PB, e.g., PB_i, where $0 \leq M \leq N$.

The adaptive beamforming strategy of PB_i is given as follows. If no sector of PB_i is active ($M = 0$), PB_i works as an omnidirectional antenna that radiates energy equally in all directions (to help power SNs outside the charging region). If at least one sector of PB_i is active ($M \geq 1$), PB_i generates M equal-power energy beams in the directions of the M active sectors. From an SN's point of view, the received power from the PBs is discussed as follows. An SN can be intentionally and efficiently charged by one or more PBs whose charging regions cover its location. When an SN is located outside the charging regions of the PBs, the SN still receives RF energy from the PBs if it is aligned with the energy radiation directions of the PBs.

We further explain the proposed AD-WPT scheme with the example of $N = 4$ in Fig. 1. It is observed that PB_1 detects three nearby sensors, i.e., SN_1, SN_2 and SN_3, which fall into three out of four sectors of its charging region. As a result, PB_1 adaptively generates three energy beams in the directions of north-east, north-west and south-west to directionally charge the three sensors. At the same time, PB_2 detects three sensors, i.e., SN_3, SN_4 and SN_5, which fall into two sectors of its charging region, and thus two adaptive energy beams are generated towards these SNs. In particular, SN_3 is within the overlapping area of the charging regions of PB_1 and PB_2, is thus intentionally charged by the two PBs at the same time. SN_1 is intentionally charged by PB_1 while it also receives energy from PB_2 and PB_3 since its location is aligned with the south-west energy radiation directions the two PBs.

B. Antenna Gain under AD-WPT

When a PB is directional, the power intensity in the directions of energy beams improves compared to the case when the PB is omnidirectional. The ratio of power intensity between directional and omnidirectional antenna is defined as the gain of directional antenna G ($G \geq 1$) [13]. In the unintended directions of the directional PB, the power intensity is zero. In the following, we evaluate G given that M out of N sectors of the PB are active.

If none of the sectors of a PB is active ($M = 0$), as discussed, the PB behaves as an omnidirectional antenna with the uniform gain in all directions, i.e.,

$$G_M = 1, \text{ for } M = 0. \tag{1}$$

If M out of N sectors of the PB are active ($M \geq 1$), the PB forms M ($M \leq N$) energy beams with equal power in the direction of each beam.[1] By the law of conservation of energy, the power intensity in the intended directions becomes N/M times of that of the omnidirectional antenna. Therefore, given M energy beams at the PB, the antenna gain in the direction of each energy beam is approximated as

$$G_M = N/M, \text{ for } M = 1, \cdots, N. \tag{2}$$

The charging radius ρ is a decision variable for the AD-WPT design. As $\rho \to 0$ or $\rho \to \infty$, all PBs in AD-WPT radiate energy in N beams with uniform gain $G_0 = G_N = 1$ as omnidirectional WPT since no SN ($M = 0$) or all SNs ($M = N$) are inside the charging regions, respectively. As ρ increases from 0 to ∞, it becomes more likely to include more SNs inside the charging region, which activates more sectors of the PB. The directional antenna gain G_M of most PBs increases sharply from $G_0 = 1$ to $G_1 = N$ and then decreases from $G_1 = N$, $G_2 = \frac{N}{2}$, $\cdots$, to $G_N = 1$. To achieve optimal AD-WPT, the design of ρ is crucial and will be discussed in Section IV.

[1]For simplicity, we assume the side lobes are negligible and the radiated energy is uniformly distributed across each energy beam.

III. Characterization of Received Power Using Stochastic Geometry

In this section, we first study the aggregate received power at a typical SN from all PBs and then use stochastic geometry to analyze the distribution of the received power.

Consider a typical sensor node SN_0 at the origin and an arbitrary PB_i at location X_i. If PB_i radiates energy with gain G_M (for $M = 0, 1, \cdots, N$) towards SN_0, the received power at SN_0 from PB_i is [14]

$$P_s^i = P_p G_M \sigma \left[\max\left(\|X_i\|/d_0, 1\right)\right]^{-\alpha}, \tag{3}$$

where P_p is the transmit power of PB_i, α is the path loss exponent, σ is a unitless constant depending on the receiver energy convention efficiency, antenna characteristics and average channel attenuation.[2] The Euclidian distance between PB_i and SN_0 is represented by $\|X_i\|$, and d_0 is a reference distance for the antenna far field. The received power from each PB is taken by averaging over the short-term fading. We adopt the non-singular path loss model [4] to avoid $\left[\|X_i\|/d_0\right]^{-\alpha} > 1$ for $\|X_i\| < d_0$. Without of the loss of generality, we use $d_0 = 1$ throughout the paper.

Equation (3) holds if PB_i radiates energy with gain G_M towards SN_0, where G_M is given in (1) or (2) depending on the number M of active sectors of PB_i. By considering all PBs in the network, the aggregate received power at SN_0 is

$$P_s = \sum_{X_i \in \Phi_p} P_s^i \mathbb{1}\left(\text{SN}_0 \text{ receives energy from } \text{PB}_i \text{ with } G_M\right).$$

The indicator function equals one if both the following conditions are satisfied:

- Condition 1: PB_i has M active sectors;
- Condition 2: SN_0 is in one of the M radiation directions of PB_i given PB_i has M active sectors.

We see that both conditions are related to the distance between SN_0 and PB_i. If SN_0 is inside the charging region of PB_i, PB_i generates at least one beam towards SN_0 ($M \geq 1$). If SN_0 is outside the charging region of PB_i, SN_0 may not be in the radiation direction of PB_i and M may vary from 0 to N.

According to the distance between PB_i and SN_0, we classify the PBs into two groups: *near* PBs with $\|X_i\| \leq \rho$, and *far* PBs with $\|X_i\| > \rho$. We draw an equivalent charging region centered at SN_0 with radius ρ and denote $b(o, \rho)$ and $\overline{b(o, \rho)}$ as the regions inside and outside this charging region, respectively. We define two indicator functions θ_n^M and θ_f^M to describe the events that SN_0 receives power from the PB with G_M conditioned on this PB is a near PB or far PB, respectively, i.e.,

$$\theta_n^M = \mathbb{1}\left[\text{SN}_0 \text{ receives energy from } \text{PB}_i \text{ with } G_M \mid \|X_i\| \leq \rho\right]$$

and

$$\theta_f^M = \mathbb{1}\left[\text{SN}_0 \text{ receives energy from } \text{PB}_i \text{ with } G_M \mid \|X_i\| > \rho\right]$$

[2]For empirical approximation, σ is sometimes set to free-space path loss at distance d_0 assuming omnidirectional antennas, i.e., $\sigma = 20 \log_{10} \frac{\nu}{4\pi d_0}$ dB [14], where ν is the wavelength of the radio waves.

where subscripts n and f denote the near and far PBs and superscript M denotes the number of active sectors of the PB.

We denote $P_{s,n}$ as the aggregate received power from the near PBs and $P_{s,f}$ as the aggregate received power from the far PBs that radiate energy towards SN_0. By summing them up, we rewrite P_s as

$$P_s = P_{s,n} + P_{s,f}, \tag{4}$$

where

$$P_{s,n} = P_p \sigma \sum_{X_i \in \Phi_p \bigcap b(o,\rho)} G_M \theta_n^M \left[\max\left(\|X_i\|, 1\right)\right]^{-\alpha}$$

and

$$P_{s,f} = P_p \sigma \sum_{X_i \in \Phi_p \bigcap \overline{b(o,\rho)}} G_M \theta_f^M \left[\max\left(\|X_i\|, 1\right)\right]^{-\alpha}.$$

As a special case of $N = 1$, all PBs are omnidirectional radiators with gain of 1. The aggregate received power at SN_0 from all omnidirectional PBs is

$$P_s^{omni} = P_p \sigma \sum_{X_i \in \Phi_p} \left[\max\left(\|X_i\|, 1\right)\right]^{-\alpha}. \tag{5}$$

To fully characterize the received power distribution, we derive the Laplace transform by taking the privilege of the independent thinning [5] of the network. For the near PBs and the far PBs, respectively, we thin the heterogeneous network into multiple homogeneous networks with certain probabilities, where in each homogeneous network the PBs radiate energy towards SN_0 with the same gain G_M ($M = 1, \cdots, N$ for the near PBs and $M = 0, 1, \cdots, N$ for the far PBs). After analyzing the Laplace transform of the received power distribution from each homogeneous network, we finally derive that from all PBs at SN_0.

A. Power Reception Probability given PB Location

First, we derive the thinning probabilities of the near PBs and the far PBs. As discussed previously, SN_0 receives power from PB_i with gain G_M if both Conditions 1 and 2 are satisfied. As for Condition 1, PB_i transmits with gain G_M if it has M active sectors. We derive the active probability of each sector as follows. As SNs follow PPP with density λ_s, the number of SNs inside a charging region is a Poisson random variable with mean $\lambda_s \pi \rho^2$. When the charging region is equally partitioned into N sectors, the number of SNs inside one of these N sectors is also a Poisson random variable, denoted by l, with mean $\lambda_s \pi \rho^2 / N$, and the probability mass function is given by

$$\Pr\left(l = \kappa\right) = \frac{\left(\lambda_s \pi \rho^2 / N\right)^{\kappa}}{\kappa!} \exp\left(-\lambda_s \pi \rho^2 / N\right), \ \kappa = 0, 1, \cdots$$

The probability that no SN is inside a sector is thus

$$p = \Pr\left(l = 0\right) = \exp\left(-\lambda_s \pi \rho^2 / N\right). \tag{6}$$

Therefore, the active probability of a sector is the probability that at least one SN is inside this sector, which is given by

$$q = 1 - p = 1 - \exp\left(-\lambda_s \pi \rho^2 / N\right). \tag{7}$$

Denote η_n^M and η_f^M as the conditional probabilities that SN_0 receives energy from PB_i with antenna gain G_M given PB_i is a near PB and a far PB, respectively. Based on p, q, Conditions 1 and 2, we derive η_n^M and η_f^M as follows.

1) Near PBs: If $\|X_i\| \leq \rho$, PB_i radiates energy in at least the direction towards SN_0 ($M \geq 1$). Condition 2 is thus satisfied. Then, η_n^M is equivalent to the probability that the rest $M-1$ out of $N-1$ sectors of PB_i have SNs, which is given as follows.

Lemma 1: Given PB_i is a near PB, the conditional probability that SN_0 receives energy from PB_i with gain G_M is

$$\eta_n^M = \binom{N-1}{M-1} p^{N-M} q^{M-1}, \text{ for } M = 1, \cdots, N. \quad (8)$$

2) Far PBs: If $\|X_i\| > \rho$, PB_i may not radiate energy towards SN_0 ($M = 0, \cdots, N$). SN_0 receives energy from PB_i with G_M if both Conditions 1 and 2 are satisfied. Then, η_f^M equals the joint probability of the event that M out of N sectors of PB_i have SNs and the event that SN_0 is in a radiation direction of PB_i. We thus obtain the following lemma (proof is omitted for brevity).

Lemma 2: Given PB_i is a far PB, the conditional probability that SN_0 receives energy from PB_i with gain G_M is

$$\eta_f^M = \begin{cases} p^N, & \text{for } M = 0 \quad (9a) \\ \dfrac{M}{N}\binom{N}{M} p^{N-M} q^M, & \text{for } M = 1, \cdots, N. \quad (9b) \end{cases}$$

B. Characterization of Received Power via Laplace Transform

In this subsection, we derive the Laplace transform of the distribution of P_s to characterize the received power at SN_0.

Define Φ_p^M as the set of PBs with gain G_M and $\Phi_p^{'}$ as the set of PBs that radiate energy towards SN_0. The set of near PBs within $b(o,\rho)$ that radiate energy with gain G_M towards SN_0 is

$$\Phi_{p,n}^M = \Phi_p^M \bigcap \Phi_p^{'} \bigcap b(o,\rho), \text{ for } M = 1, \cdots, N, \quad (10)$$

which is obtained through the independent thinning [5] of near PBs with new density $\lambda_p \eta_n^M$, where η_n^M is given in Lemma 1. Similarly, the set of far PBs within $\overline{b(o,\rho)}$ that radiate energy with gain G_M towards SN_0 is

$$\Phi_{p,f}^M = \Phi_p^M \bigcap \Phi_p^{'} \bigcap \overline{b(o,\rho)}, \text{ for } M = 0, \cdots, N, \quad (11)$$

which by the independent thinning of far PBs with new density $\lambda_p \eta_f^M$, where η_f^M is given in Lemma 2. Note that SN_0 receives zero power from the far PBs that does not radiate energy towards SN_0.

We rewrite the aggregate received power at SN_0 from all the near PBs and far PBs in (4) as

$$P_s = P_{s,n} + P_{s,f} = \sum_{M=1}^{N} P_{s,n}^M + \sum_{M=0}^{N} P_{s,f}^M, \quad (12)$$

where

$$P_{s,n}^M = P_p \sigma \sum_{X_i \in \Phi_{p,n}^M} G_M \left[\max\left(\|X_i\|, 1\right)\right]^{-\alpha} \quad (13)$$

is the aggregate received power from the near PBs with gain G_M and

$$P_{s,f}^M = P_p \sigma \sum_{X_i \in \Phi_{p,f}^M} G_M \left[\max\left(\|X_i\|, 1\right)\right]^{-\alpha} \quad (14)$$

is the aggregate received power from the far PBs with gain G_M. Since we adopt the non-singular path loss function $\left[\max\left(\|X_i\|, 1\right)\right]^{-\alpha}$, our analysis involves two cases: $0 < \rho \leq 1$ and $1 < \rho < \infty$. Define $\gamma(s,x) = \int_0^x t^{s-1} e^{-t} dt$ as the lower incomplete gamma function. The Laplace transforms of the distributions of $P_{s,n}^M$ and $P_{s,f}^M$ are given as follows.

Lemma 3: The Laplace transform of the distribution of aggregate received power at the typical SN_0 from the near PBs with gain G_M is

$$\mathcal{L}_{P_{s,n}^M}(s) = \begin{cases} \mathcal{L}_{P_{s,n}^M(1)}(s), & \text{for } 0 < \rho \leq 1 \quad (15a) \\ \mathcal{L}_{P_{s,n}^M(2)}(s), & \text{for } 1 < \rho < \infty, \quad (15b) \end{cases}$$

where

$$\mathcal{L}_{P_{s,n}^M(1)}(s) = \exp\left\{ -\lambda_p \pi \eta_n^M \left[\rho^2 - \rho^2 \exp\left(-s P_p \sigma G_M\right)\right] \right\} \quad (16)$$

and

$$\begin{aligned} \mathcal{L}_{P_{s,n}^M(2)}(s) &= \exp\Bigg\{ -\lambda_p \pi \eta_n^M \Bigg\{ \rho^2 - \rho^2 \exp\left(-s P_p \sigma G_M \rho^{-\alpha}\right) \\ &\quad + \left(s P_p \sigma G_M\right)^{\frac{2}{\alpha}} \Bigg[\gamma\left(1 - \frac{2}{\alpha}, s P_p \sigma G_M\right) \\ &\quad - \gamma\left(1 - \frac{2}{\alpha}, s P_p \sigma G_M \rho^{-\alpha}\right) \Bigg] \Bigg\} \Bigg\}. \end{aligned} \quad (17)$$

Lemma 4: The Laplace transform of the distribution of aggregate received power at the typical SN_0 from the far PBs with gain G_M is

$$\mathcal{L}_{P_{s,f}^M}(s) = \begin{cases} \mathcal{L}_{P_{s,f}^M(1)}(s), & \text{for } 0 < \rho \leq 1 \quad (18a) \\ \mathcal{L}_{P_{s,f}^M(2)}(s), & \text{for } 1 < \rho < \infty, \quad (18b) \end{cases}$$

where

$$\begin{aligned} \mathcal{L}_{P_{s,f}^M(1)}(s) &= \exp\Bigg\{ \lambda_p \pi \eta_f^M \Bigg\{ \rho^2 - \rho^2 \exp\left(-s P_p \sigma G_M\right) \\ &\quad - \left(s P_p \sigma G_M\right)^{\frac{2}{\alpha}} \gamma\left(1 - \frac{2}{\alpha}, s P_p \sigma G_M\right) \Bigg\} \Bigg\} \end{aligned} \quad (19)$$

and

$$\begin{aligned} \mathcal{L}_{P_{s,f}^M(2)}(s) &= \exp\Bigg\{ \lambda_p \pi \eta_f^M \Bigg\{ \rho^2 - \rho^2 \exp\left(-s P_p \sigma G_M \rho^{-\alpha}\right) \\ &\quad - \left(s P_p \sigma G_M\right)^{\frac{2}{\alpha}} \gamma\left(1 - \frac{2}{\alpha}, s P_p \sigma G_M \rho^{-\alpha}\right) \Bigg\} \Bigg\}. \end{aligned} \quad (20)$$

Proof: Due to the space limitation, the proofs of the above two lemmas are omitted and will be presented in Appendix A and B of the journal version [15]. ■

Based on Lemma 3 and Lemma 4, we obtain the Laplace transform of the distribution of P_s in the following proposition.

Proposition 1: The Laplace transform of the distribution of aggregate received power at the typical SN_0 from all PBs under AD-WPT is given by

$$\mathcal{L}_{P_s}(s) = \begin{cases} \prod_{M=1}^{N} \mathcal{L}_{P^M_{s,n}(1)}(s) \prod_{M=0}^{N} \mathcal{L}_{P^M_{s,f}(1)}(s), \text{for } 0<\rho\leq 1 \\ \prod_{M=1}^{N} \mathcal{L}_{P^M_{s,n}(2)}(s) \prod_{M=0}^{N} \mathcal{L}_{P^M_{s,f}(2)}(s), \text{ for } \rho>1. \end{cases}$$

As a special case of $N=1$, the Laplace transform of the distribution of aggregate received power at SN_0 from all PBs in omnidirectional WPT is given by

$$\mathcal{L}_{P_s^{omni}}(s) = \exp\left\{ -\lambda_p \pi (sP_p\sigma)^{\frac{2}{\alpha}} \gamma\left(1-\frac{2}{\alpha}, sP_p\sigma\right)\right\}.$$

Proof:

$$\begin{aligned}\mathcal{L}_{P_s}(s) &= \mathbb{E}\left[\exp\left(-sP_s\right)\right] \\ &= \mathbb{E}\left[\exp\left(-s\sum_{M=1}^{N} P^M_{s,n}\right)\right]\mathbb{E}\left[\exp\left(-s\sum_{M=0}^{N} P^M_{s,f}\right)\right] \\ &= \prod_{M=1}^{N}\mathbb{E}\left[\exp\left(-sP^M_{s,n}\right)\right]\prod_{M=0}^{N}\mathbb{E}\left[\exp\left(-sP^M_{s,f}\right)\right] \\ &= \prod_{M=1}^{N}\mathcal{L}_{P^M_{s,n}}(s)\prod_{M=0}^{N}\mathcal{L}_{P^M_{s,f}}(s) \end{aligned} \quad (22)$$

■

IV. Maximization of Average Received Power in AD-WPT

In this section, we analyze the average received power $\mathbb{E}[P_s]$ at the typical SN_0 and derive the optimal charging region radius ρ that maximizes $\mathbb{E}[P_s]$. The average received power at SN_0 is given by

$$\mathbb{E}[P_s] = -\frac{d}{ds}\left[\log\left(\mathcal{L}_{P_s}(s)\right)\right]|_{s=0}. \quad (23)$$

This is the expectation of the aggregate received power at SN_0 from all PBs by taking over all possible location realizations of the PBs in spatial domain. By further derivations, the results are summarized in the following proposition.

Proposition 2: At the typical SN_0, the average received power in AD-WPT is given by

$$\mathbb{E}[P_s] = \begin{cases} P_p\lambda_p\sigma\pi\left[\frac{\rho^2\left(p-p^N\right)}{1-p}+\frac{\alpha}{\alpha-2}\right], \\ \qquad\qquad \text{for } 0<\rho\leq 1 \quad (24a) \\ P_p\lambda_p\sigma\pi\left[\frac{\left(\alpha-2\rho^{2-\alpha}\right)\left(1-p^N\right)}{(\alpha-2)(1-p)}\right. \\ \qquad \left.+\frac{2\rho^{2-\alpha}}{\alpha-2}\right], \text{ for } 1<\rho<\infty, \quad (24b) \end{cases}$$

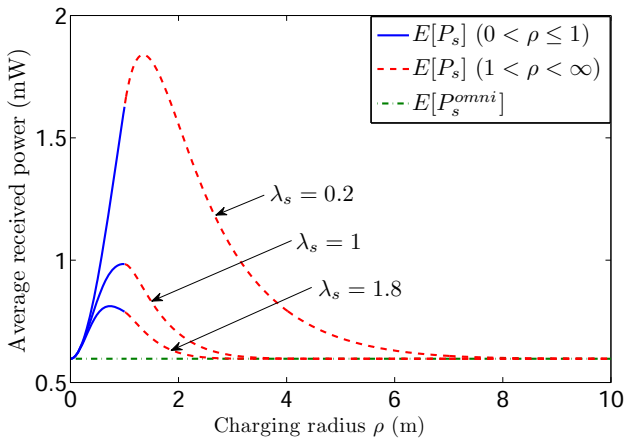

Fig. 2. Average received power versus charging radius ($P_p = 10$ W, $\nu = 0.1$ m, $\alpha = 3$, $\lambda_p = 0.1$ and $N = 8$).

where p is given in (6) and $\mathbb{E}(P_s)$ is continuous at $\rho = 1$. As a special case of $N=1$, the average received power at SN_0 in omnidirectional WPT is given by

$$\mathbb{E}[P_s^{omni}] = \frac{P_p\lambda_p\sigma\pi\alpha}{\alpha-2}. \quad (25)$$

For $0<\rho<\infty$, it follows that $\mathbb{E}[P_s] > \mathbb{E}[P_s^{omni}]$. For $\rho\to 0$ and $\rho\to\infty$, we have $\mathbb{E}[P_s]\to\mathbb{E}[P_s^{omni}]$.

Proof: The proofs are omitted due to the lack of space. See Appendix C and D of the journal version [15]. ■

In Proposition 2, the average received power in AD-WPT outperforms that in omnidirectional WPT for all ρ. For any given ρ, $\mathbb{E}[P_s]$ is increasing with the increased P_p, λ_p and N and is decreasing with the increased λ_s. Moreover, for any given set of $\{P_p, \lambda_p, \lambda_s, N\}$, $\mathbb{E}[P_s]$ is unimodal in ρ, i.e., $\mathbb{E}[P_s]$ first increases and then decreases with the increased ρ and there exists a unique ρ^* that maximizes $\mathbb{E}[P_s]$ as shown in Fig. 2. When ρ increases from 0 to ∞, the power intensity of most PBs increases and then decreases with the increased of ρ (as discussed in Section II-B), which therefore improves and reduces $\mathbb{E}[P_s]$, respectively.

In the following, we study the optimal charging radius ρ^* that maximizes $\mathbb{E}[P_s]$ in Proposition 2, i.e.,

$$\text{P1}: \quad \mathbb{E}[P_s]^* = \max_{0<\rho<\infty} \mathbb{E}[P_s]. \quad (26)$$

As shown in Fig. 2, the optimal ρ^* is the single stationary point of $\mathbb{E}[P_s]$. Moreover, $\mathbb{E}[P_s]$ decreases with the increased λ_s. For small λ_s (e.g., $\lambda_s = 0.2$), $\rho^* \in (1,\infty)$ is the stationary point of (24b). For large λ_s (e.g., $\lambda_s = 1.8$), $\rho^* \in (0,1]$ is the stationary point of (24a). It can be proved that $D_1(\rho) = \frac{\partial[\mathbb{E}[P_s]|_{0<\rho\leq 1}]}{\partial\rho}$ and $D_2(\rho) = \frac{\partial[\mathbb{E}[P_s]|_{1<\rho<\infty}]}{\partial\rho}$ are of the same sign at the point of $\rho = 1$. The procedure to obtain the optimal ρ^* is summarized in Algorithm 1.

V. Numerical Results

In this section, we present the simulation results of the proposed AD-WPT scheme, compared with the omnidirectional WPT as a performance benchmark. We set $\sigma = -41.9842$ dB,

Algorithm 1 Solving the optimal charging radius in P1:

1: Calculate $D_1(\rho)$ and $D_2(\rho)$
2: **if** either $D_1(\rho=1)<0$ or $D_2(\rho=1)<0$ **then**
3: ρ^* is the solution to $D_1(\rho)=0$
4: **else if** either $D_1(\rho=1)=0$ or $D_2(\rho=1)=0$ **then**
5: $\rho^*=1$
6: **else if** either $D_1(\rho=1)>0$ or $D_2(\rho=1)>0$ **then**
7: ρ^* is the solution to $D_2(\rho)=0$
8: **end if**

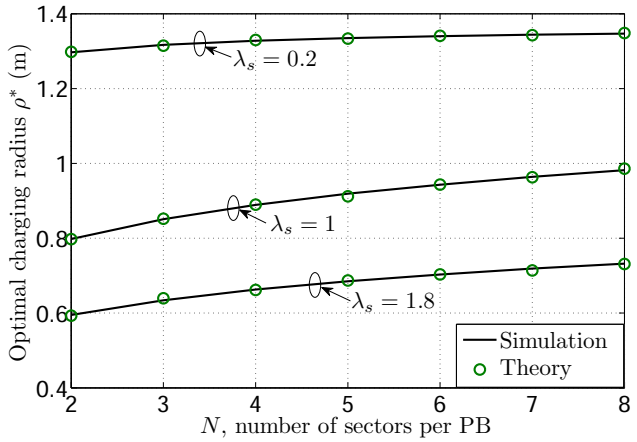

Fig. 3. Optimal charging radius ρ^* for average power maximization versus N ($\lambda_p = 0.1$, $P_p = 10$ W and $\alpha = 3$).

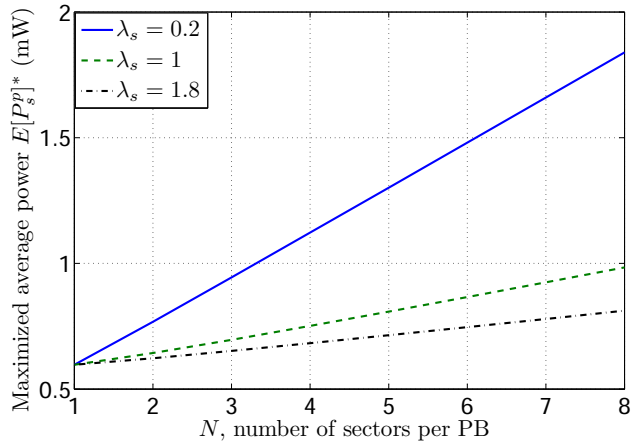

Fig. 4. Maximized average received power $\mathbb{E}[P_s]^*$ versus N ($\lambda_p = 0.1$, $P_p = 10$ W and $\alpha = 3$).

where the wavelength is $\nu = 0.1$ m and the reference distance is $d_0 = 1$ m. Fig. 3 and Fig. 4 show that both the maximized average received power $\mathbb{E}[P_s]^*$ and the corresponding optimal charging radius ρ^* increase with the increased number of PB sectors N. For $N = 1$, AD-WPT is equivalent to omnidirectional WPT. As N increases, the PBs are able to form narrower energy beams with higher power intensity towards the intended SNs. As a result, the coverage of PBs in AD-WPT extends and it is more beneficial to use a larger charging radius ρ^* as shown in Fig. 3 to serve more SNs efficiently. As for the optimal ρ^*, the simulation results match well with the theoretical results given by Algorithm 1. With the decreased beamwidth, the power intensity of the PBs increases, which thus improves $\mathbb{E}[P_s]^*$ as shown in Fig. 4. We also observe that ρ^* and $\mathbb{E}[P_s]^*$ decrease with the increased SN density λ_s. As λ_s increases, the power intensity of most PBs decreases due to the increased number of energy beams. As a result, the PBs shrink the charging radius in AD-WPT to serve fewer SNs efficiently as shown in Fig. 3. $\mathbb{E}[P_s]^*$ decreases with the increased λ_s due to the decreased power intensity of the PBs as shown in Fig. 4.

VI. Conclusions

In this paper, we proposed an AD-WPT scheme in a large-scale sensor network, where the PBs charge the SNs by adapting the energy beamforming strategies to the nearby SN locations. By using stochastic geometry, we derived the closed-form expression of the aggregate received power distribution at the typical SN. The optimal radius was designed to maximize the average received power. The results show that both the optimal charging radius and maximized average received power decrease with the increased energy beamwidth and density of the SNs. Moreover, the optimal AD-WPT is more energy efficient than omnidirectional WPT by achieving equivalent average received power with less transmit power at PBs.

References

[1] I. Akyildiz, W. Su, Y. Sankarasubramaniam, and E. Cayicrci, "A survey on sensor networks," *IEEE Commun. Mag.*, vol. 40, no. 8, pp. 102-114, Aug. 2002.

[2] S. Bi, C. K. Ho, and R. Zhang, "Wireless powered communication: opportunities and challenges," *IEEE Commun. Mag.*, vol. 53, no. 4, pp. 117-125, Apr. 2015.

[3] M. Erol-Kantarci and H. T. Mouftah,, "Suresense: sustainable wireless rechargeable sensor networks for the smart grid," *IEEE Wireless Commun.*, vol. 19, no. 3, pp. 30-36, Jun. 2012.

[4] M. Haenggi and R. K. Ganti, *Interference in Large Wireless Networks,* Now Publishers, 2008.

[5] D. Stoyan, W. Kendall, and J. Mecke, *Stochastic Geometry and its Applications, 2nd Edition,* Wiley, 1995.

[6] X. Zhou, R. Zhang, and C. K. Ho, "Wireless information and power transfer: architecture design and rate-energy tradeoff," *IEEE Trans. Commun.,* vol. 61, no. 11, pp. 4757-4767, Nov. 2013.

[7] H. Ju and R. Zhang, "Throughput maximization in wireless powered communication networks," *IEEE Trans. Wireless Commun.,* vol. 13, no. 1, pp. 418-428, Jan. 2014.

[8] S. H. Lee, R. Zhang, and K. B. Huang, "Opportunistic wireless energy harvesting in cognitive radio networks," *IEEE Trans. Wireless Commun.,* vol. 12, no. 9, pp. 4788-4799, Sep. 2013.

[9] Y. L. Che, L. Duan, and R. Zhang, "Spatial throughput maximization in large scale wireless powered communication networks," *IEEE J. Sel. Areas in Commun.,* to appear.

[10] J. Xu and R. Zhang, "Energy beamforming with one-bit feedback," *IEEE Trans. Sig. Process.,* vol. 62, no. 20, pp. 5370-5381, Oct. 2014.

[11] R. Zhang and C. K. Ho, "MIMO broadcasting for simultaneous wireless information and power transfer," *IEEE Trans. Wireless Commun.,* vol. 12 , no. 5, pp. 1989-2001, May 2013.

[12] K. Huang and V. K. N. Lau, "Enabling wireless power transfer in cellular networks: Architecture, modeling and deployment," *IEEE Trans. Wireless Commun.*, vol. 13, no. 2, pp. 902-912, Feb. 2014.

[13] C. A. Balanis, *Antenna Theory: Analysis and Design (3rd),* Wiley, 2005.

[14] A. Goldsmith, *Wireless Communications,* Cambridge. University Press, 2005.

[15] Z. Wang, L. Duan, and R. Zhang, "Adaptively directional wireless power transfer for large-scale sensor networks," submitted, 2015.